Hydra Probe and Twelve-Wire Probe Comparisons in Fluids and Soil Cores

S. D. Logsdon*
USDA-ARS
National Laboratory for Agriculture and the Environment
2110 University Boulevard
Ames, IA 50011

T. R. Green
USDA-ARS
Agricultural Systems Research Unit
Fort Collins, CO

M. Seyfried
USDA-ARS
Northwest Watershed Research Center
Boise, ID

S. R. Evett
USDA-ARS
Soil and Water Research
Bushland, TX

J. Bonta
USDA-ARS
North Appalachian Experimental Watershed
Coshocton, OH

Soil water content is often determined using various permittivity sensors. The Hydra Probe reports both the real (ε') and imaginary (ε'') components of complex permittivity (ε^*) and estimates electrical conductivity (σ'). Previously, a 12-wire probe was used with a vector network analyzer to determine ε' and ε'' and σ' and σ'' in undisturbed soil cores. The purpose of this study was to compare results from the Hydra Probe and the 12-wire probe for fluids as well as for soil samples taken from six locations, to better understand the interrelations of ε', ε'', and σ' from the Hydra Probe. Undisturbed soil cores were collected from an Iowa prairie and adjacent soybean [*Glycine max* (L.) Merr.] field, an Iowa forest and adjacent soybean field, Idaho burned and unburned sites, Colorado grassland and dryland wheat (*Triticum aestivum* L.) sites, Ohio grassed areas, and Texas rangeland and an irrigated field. Because of their density, some of the Texas samples were sieved and repacked. The reported σ', ε', and ε'' values of fluids were compared between the two measurement systems and with theoretical values. Because the theoretical values for soils are not known, the measured values were compared between systems. Both probes showed σ', ε', and ε'' close to the theoretical values for fluids. In soils, we showed that an adjustment was needed in the calculated σ' from the Hydra Probe to account for dielectric relaxation. The soil σ' of the Hydra Probe matched σ' from the 12-wire probe better after the adjustment was made.

Abbreviations: VNA, vector network analyzer.

Accurate soil water content data are needed for evaluating the efficiency of soil water use and for understanding soil water flow in the landscape. Automated soil water sensors infer the temporal dynamics of water content in the soil as part of the soil–plant–atmosphere continuum (McCoy et al., 2006). Many of these sensors are based on a relationship between permittivity and water content (θ). The assumption for using dielectric sensors to determine θ is based on known properties for free water, minerals, and air. Most sensors have a measurement frequency (f) in the megahertz to low gigahertz range, below the permittivity relaxation frequency (f_{rel}) for free water (~17 GHz); therefore, the assumption is often made that the permittivity of pure water is relatively constant at the low-f value (76–80 depending on temperature).

Permittivity is complex (ε^*), with real (ε') and imaginary (ε'') components. The ε'' is affected by direct current electrical conductivity (σ_{dc}) as well as a relaxation component (ε_{rel}''), whereas ε' is only affected by a relaxation component:

$$\varepsilon^* = \varepsilon' - i\left(\varepsilon_{rel}'' + \frac{\sigma_{dc}}{2\pi f \varepsilon_v}\right) \quad [1]$$

where ε_v is the permittivity of a vacuum (8.854×10^{-12} F m^{-1}). Electrical conductivity is also complex (σ^*), with real (σ') and imaginary (σ') components. The σ_{dc} is usually inferred by measuring σ'' under a small measurement frequency (f) of alternating current in which the value is only slightly larger than σ_{dc}. Many soil moisture probes determine apparent permittivity (ε_a) rather than ε'. The ε'' makes a strong contribution to $\varepsilon_a^{1/2}$:

$$\varepsilon_a^{1/2} = \sqrt{\frac{\varepsilon'}{2}\left[1 + \sqrt{1 + \left(\frac{\varepsilon''}{\varepsilon'}\right)^2}\right]} \quad [2]$$

Soil Sci. Soc. Am. J. 74:5–12
Published online 13 Nov. 2009.
doi:10.2136/sssaj2009.0189
Received 12 May 2009.
*Corresponding author (sally.logsdon@ars.usda.gov).
© Soil Science Society of America, 677 S. Segoe Rd., Madison WI 53711 USA
All rights reserved. No part of this periodical may be reproduced or transmitted in any form or by any means, electronic or mechanical, including photocopying, recording, or any information storage and retrieval system, without permission in writing from the publisher. Permission for printing and for reprinting the material contained herein has been obtained by the publisher.

Many soil water probes (e.g., Blonquist et al., 2005; Logsdon and Hornbuckle, 2006) operate at lower f than time domain reflectometry (TDR), but do not require waveform analysis. The lower f permittivity values are more subject to influences beyond those of "free" water. Soils high in smectite clays have extra apparent σ' due to "proton hopping" (Poinsignon, 1997; Hunt et al., 2006). Proton hopping refers to charge transfer through interlayer water in the 2:1 smectite clays in response to an applied alternating current, which is implicit in any of the TDR or other permittivity sensing systems. The high σ' contributes to larger than expected values for $\varepsilon_a^{1/2}$ at lower f.

Overall, ε'' is more strongly increased at lower f than is ε' (Logsdon and Hornbuckle, 2006; Seyfried and Grant, 2007). The increased ε'' results in $\varepsilon_a^{1/2}$ being larger and more related to soil variation than is ε'; therefore, ε' should correlate better with θ across a range of soils. Many sensors also may be affected by non-uniform soil water distribution (Logsdon, 2009; Evett et al., 2009).

Other mechanisms have been suggested to increase $\varepsilon_a^{1/2}$ at even lower frequencies, including soil–sensor interactions (electrode polarization, Schwan, 1966) and other polarization effects that are more prominent in slurries (Raythatha and Sen, 1986; Ishida and Makino, 1999; Bialkowski et al., 2002; Ishida et al., 2003) than in moist soil. The mixing models used to describe these polarization effects do not always include particle-to-particle interaction, which may be not be needed for slurries but is essential for moist soil, in which the particles are closely spaced. These other mechanisms are not considered further here because shape factors are unknown, and soil particle-to-particle interaction is important (Robinson et al., 2005). Only the polarization mixing models that include interaction terms may be successfully applied to moist soil (Robinson et al., 2005; Schwartz et al., 2009a,b). Schwartz et al. (2009a,b) calculated the contributions to ε^* of relaxation effects (ε_{rel}'') due to bound water in addition to the effects of σ_{dc} and f on ε^* (Eq. [1]).

Because σ' is positively affected by temperature, $\varepsilon_a^{1/2}$ is also positively related to temperature for soils with high σ', whether due to salts or to proton migration in smectite clays (Evett et al., 2005, 2006). Bound-water relaxation and the other processes mentioned above also contribute to a positive temperature effect because f is smaller than f_{rel} (de Loor, 1968).

The Hydra Probe I (Stevens Vitel, Inc., Portland, OR) operates at about 50 MHz and reports both ε' and ε'' as well as σ' (Seyfried and Murdock, 2004). Unfortunately σ' is calculated assuming that ε'' has only the σ_{dc} component. The Hydra Probe has been observed to be less sensitive to temperature than other low-f sensors that are based only on ε_a (Blonquist et al., 2005; Logsdon and Hornbuckle, 2006), probably because σ_{dc} does not directly affect ε' as it does ε_a.

In previous work, permittivity spectra (as a function of f) were collected from soils packed into a coaxial sample holder (Logsdon, 2005, 2008a), but recent measurements were made with a 12-wire, quasi-coaxial probe (Logsdon, 2008b) that could be inserted into undisturbed soil samples. The larger volume and smaller surface area of the 12-wire probe reduced electrode polarization effects at lower frequencies, but the larger volume decreased the usable frequency range. Inserting the 12-wire probe into soil samples allowed measurement on undisturbed soil (Logsdon, 2008b).

The purpose of this study was to better understand the interrelations of ε', ε'', and σ' from the Hydra Probe by comparing Hydra Probe measurements with theory and with measurements from the 12-wire probe for both fluids and undisturbed soils taken from six locations across the United States that represent different land uses and soils.

MATERIALS AND METHODS

Soil Samples

Undisturbed soil cores were collected from Colorado, Idaho, Iowa, Ohio, and Texas (Fig. 1). The samples spanned different soils and vegetation within each state. If possible, cropping sequences were selected to represent typical cropping sequences for the area, and an alternate cropping sequence (long-term rotation, pasture, restored prairie, or forest) was included. From each combination of location, crop, and soil, we collected six undisturbed cores in thin-walled steel rings (74-mm diameter, 76 mm long). Most of the samples were taken at the soil surface, but the Texas samples were taken deeper (see below). The cores were stored at 4°C until analysis.

Site characteristics and locations are presented in Tables 1 and 2. The soils were Mollisols, Inceptisols, Entisols, Vertisols, or Ultisols. The mineralogy was generally mixed, with some soils being smectitic and others superactive or active. A few soils were coarse loamy, but most were fine textured. Some had $CaCO_3$ (Table 1).

For the Iowa prairie site, samples were taken from a restored prairie site and an adjacent corn (*Zea mays* L.)–soybean field (in the soybean year of the rotation). For the Iowa forest site, samples were taken from a forest and an adjacent field in a corn–soybean rotation.

For the Idaho site, samples were taken along a prescribed fire boundary. The unburned area was in shrub vegetation [mountain sagebrush, *Artemisia tridentata* Nutt. ssp. *vaseyana* (Rydb.) Beetle, and bitterbrush, *Purshia tridentata* (Pursh) DC.], and the burned area had regrown grass and forbs. The Ola soil was on a ridge of granite, the Kanlee soil on flat upland ~150 m lower than ridge, and the "pit" next to seasonal meadow.

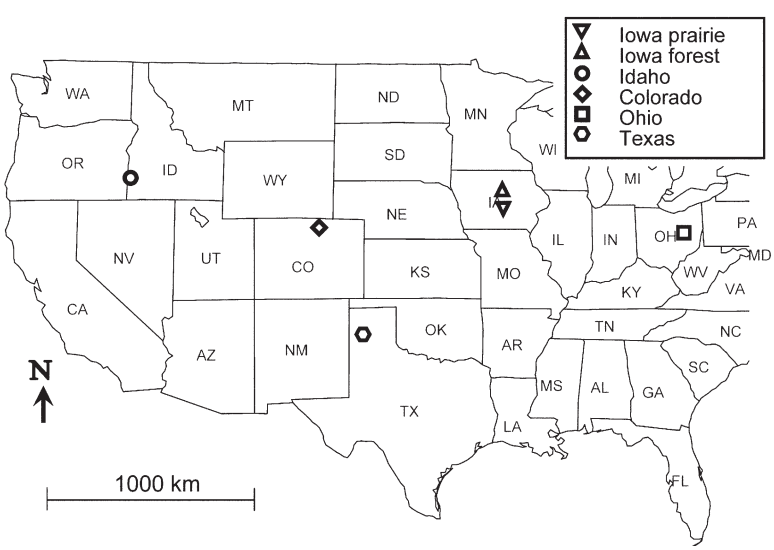

Fig. 1. Location of sites in the United States.

Table 1. Soil characterization for the sites from the different states, with mean (and standard deviation in parentheses) bulk density (BD) and sorbed water (SW).

Site	Soil	Classification†	BD	SW
			Mg m^{-3}	kg kg^{-1}
Iowa prairie	Killduff	fine-silty, mixed, superactive, mesic Dystric Eutrudept	1.22 (0.07)	0.036 (0.008)
Iowa prairie	Mahaska	fine, smectitic, mesic Aquertic Argiudoll	1.21 (0.04)	0.050 (0.006)
Iowa prairie	Tama	fine-silty, mixed, superactive, mesic Typic Argiudoll	1.15 (0.07)	0.042 (0.001)
Iowa forest	Galva	fine-silty, mixed, superactive, mesic Typic Hapludoll	1.02 (0.09)	0.061 (0.003)
Iowa forest	Sac	fine-silty, mixed, superactive, mesic Oxyaquic Hapludoll	0.97 (0.09)	0.064 (0.005)
Iowa forest	Primghar	fine-silty, mixed, superactive, mesic Aquic Hapludoll	1.00 (0.14)	0.060 (0.006)
Idaho	Ola	coarse-loamy, mixed, superactive, frigid Pachic Haploxeroll	1.14 (0.10)	0.030 (0.009)
Idaho	Kanlee	fine-loamy, mixed, superactive, frigid Typic Argixerol	1.15 (0.21)	0.032 (0.008)
Idaho	Pit, uncertain	coarse-loamy, mixed, superactive, frigid Ultic Haploxeroll	1.17 (0.14)	0.038 (0.004)
Colorado	Colby	fine-silty, mixed, superactive, calcareous, mesic Aridic Ustorthent	1.30 (0.05)	0.036 (0.001)
Colorado	Wagonwheel	coarse-silty, mixed, superactive, mesic Aridic Calciustept	1.30 (0.03)	0.034 (0.002)
Colorado	Kim	fine-loamy, mixed, active, calcareous, mesic Ustic Torriorthent	1.26 (0.05)	0.035 (0.004)
Ohio	Lordstown	coarse-loamy, mixed, active, mesic Typic Dystrudept	1.03 (0.07)	0.036 (0.001)
Ohio	Muskingum	fine-loamy, mixed, semiactive, mesic Typic Dystrudept	1.25 (0.03)	0.032 (0.001)
Ohio	Rayne	fine-loamy, mixed, active, mesic Typic Hapludult	1.24 (0.05)	0.030 (0.001)
Texas‡	Pullman	fine, mixed, superactive, thermic Torrertic Paleustoll	0.90 (0.04)	0.071 (0.004)
Texas	Randall	fine, smectitic, thermic Ustic Epiaquert	0.80 (0.03)	0.103 (0.000)
Texas	Mansker	fine-loamy, carbonatic, thermic Calcidic Paleustoll	0.97 (0.03)	0.063 (0.003)

† Classification according to Soil Survey Staff (2008).

‡ The data for the Texas samples are for repacked subsoil samples. Bulk densities for undisturbed Pullman samples were 1.12 (0.06) Mg m^{-3} for the near-surface samples and 1.26 (0.18) Mg m^{-3} for subsurface samples. The sorbed water for the undisturbed Pullman samples was 0.063 (0.005) kg kg^{-1} for near-surface samples and 0.068 (0.004) kg kg^{-1} for subsurface samples.

The samples from Colorado were taken from grassland or the fallow phase of a wheat–fallow rotation. Green et al. (2009) provided a detailed description of the Colorado site and spatial analysis of 150 steady infiltration measurements on fallow soils (mean and standard deviation of the field saturated hydraulic conductivity were 0.40 and 0.20 m d^{-1}). McCutcheon et al. (2006) explored the relationships between soil bulk electrical conductivity, texture, and water content at this field site. They mapped the Colorado soils reported here in Table 1.

The samples from Ohio were all taken from grassland or pasture because different management practices were not used on these soils. The soils were developed from sandstone and siltstone, perhaps with some loess at the surface. The Pullman soil samples were taken from rangeland and an irrigated field. The rangeland site included soils for the playa bottom (Randall series) and side (Mansker series).

The original set of Texas samples were taken at 0.3-m depth instead of at the soil surface. The soils from Texas were very dense and difficult to measure with the delicate 12-wire probe. After attempting to measure a set of samples, all the samples were removed from the core, sieved moist through an 8-mm sieve, and repacked at a lower density before analysis. Repacking was done by layers, scratching one layer before adding the next to aid continuity between layers. Because the Pullman soil was dense when sampled dry, additional undisturbed samples were taken in moist soil at 0.1- or 0.25-m centered depth.

Twelve-Wire Probe with Vector Network Analyzer

The 12-wire probe used in this study was slightly modified from an earlier version (Logsdon, 2008b). The refined 12-wire probe has 50-mm-long wires that extend 41 mm beyond the head, with a wire diameter of 2 mm. (The previous 12-wire probe had wires of 1-mm diameter, which deformed too easily.) The 13-mm-thick epoxy head surrounded the wires that connected the six inner wires (diameter of 20 mm) to the middle pin of a BNC connector, and that connected the six outer wires (diameter of 56 mm) to the outside of the BNC connector. The reason for using a 12-wire probe was to allow measurements on undisturbed soil samples and to approximate a coaxial system with probe impedance not too different from 50 Ω. The modification from the earlier version (Logsdon, 2008b) was to use 2-mm-diameter wires.

The electrical spectra data were processed, as described by Logsdon (2005), after calibration of the 12-wire probe using a calibration kit of open, short, and load attachments. Output from the vector network analyzer (VNA), the complex reflection scattering parameter (S11*), was converted (Logsdon, 2005) to complex impedance (Z^*) and complex σ^* and ε^*:

$$Z^* = 50\left(\frac{1+\mathrm{S11}^*}{1-\mathrm{S11}^*}\right) \qquad [3a]$$

$$\sigma^* = \frac{Z_p \varepsilon_v c}{L Z^*} \qquad [3b]$$

$$\varepsilon^* = \frac{\sigma^*}{\pi f \varepsilon_v \arctan\left(\frac{2\sigma'}{\sigma''}\right)} \qquad [3c]$$

Table 2. Locations of the sites sampled for this study.

Site	Latitude	Longitude	Elevation
			m
Iowa prairie	41°32′ N	93°17′ W	310
Iowa forest	42°26′ N	95°9′ W	310
Idaho	43°6′ N	116°46′ W	1590
Colorado	40°36′ N	10°50′ W	1575
Ohio	40°21′ N	81°47′ W	350
Texas	35°11′ N	102°6′ W	1170

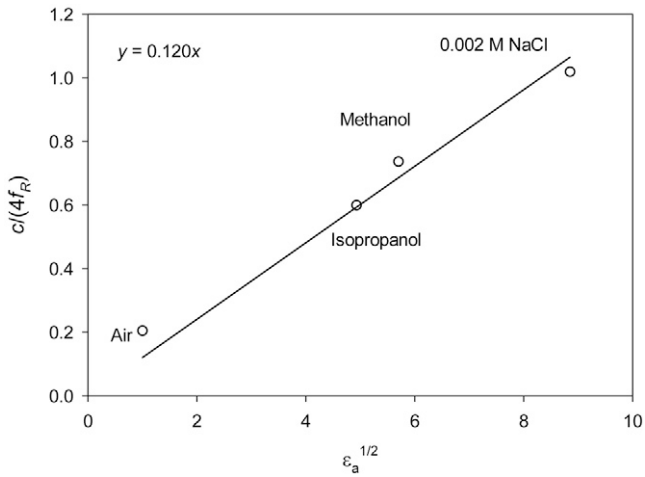

Fig. 2. Fluid calibration to determine the electrical length (0.12 m) of the new 12-wire probe, with a physical length of 0.041 m. Plotting the square root of the apparent permittivity ($\varepsilon_a^{1/2}$) as a function of $c/4f_R$ results in a slope of $1/L$, where c is the speed of light, f_R is the resonance frequency, and L is the electrical length (m).

where Z_p is the probe impedance in air (calculated from the probe dimensions):

$$Z_p = \frac{60}{\varepsilon^*} \ln\left(\frac{m}{k}\right) \qquad [4]$$

where c is the speed of light, L is the electrical length (Berberian and King, 2002), and m and k are the outer and inner radii of the coaxial cell. Combining Eq. [1] and [2], ε_a is

$$\varepsilon_a = \frac{\varepsilon'}{2}\left[1+\sqrt{1+\left(\frac{\varepsilon_{rel}'' + \sigma_{dc}/2\pi f \varepsilon_v}{\varepsilon'}\right)^2}\right] \qquad [5]$$

The electrical length, L, was determined from the known resonance frequencies (f_R) of various fluids (Heimovaara et al., 1996; Shang et al., 1999; Logsdon, 2005):

$$\varepsilon_a^{1/2} = \frac{c}{4Lf_R} \qquad [6]$$

The f_R is the frequency at the first minimum of the real part of the scatter function (S11'). Plotting $c/(4f_R)$ as a function of theoretical ε_a for each fluid gave the L for the probe (Logsdon, 2005) as 0.12 m (Fig. 2). The extra length of wires in the head apparently add to the electrical length, which does not equal the physical length. The fluids used were air, methanol (Fellner-Feldegg, 1969; Baker-Jarvis et al., 1998), isopropanol (Baker-Jarvis et al., 1998), and a 0.002 mol L^{-1} NaCl solution (Stogryn, 1971). Equation [6] was also used to determine the $\varepsilon_a^{1/2}$ for each soil sample at f_R using the length determined from the fluid regression. In addition to σ' at 300 kHz (the lowest measurement frequency of the VNA), we fitted the spectra, $\sigma'(f)$, to determine σ_{dc}, the characteristic frequency, f_c, and the exponent, n (Hunt et al., 2006):

$$\sigma'(f) = \sigma_{dc}\left(1+\frac{f}{f_c}\right)^n \qquad [7]$$

The curves from a few of the dry samples ($\theta < 0.1$ m^3 m^{-3}) could not be fitted because f_c was lower than the lowest measured f. The f_c was used as a substitute for f_{rel} since the ε^* data did not cover a broad enough f range to determine other f_{rel} values, especially those dominating lower f values. Multiple f_{rel} values would be expected for these samples if the f range was larger.

Hydra Probe

Another soil core of each set was used with the Hydra Probe for determining ε' and ε'' at 50 MHz and σ_{dc}. The internal calculations for the Hydra Probe (Seyfried et al., 2005) are based on those of Campbell (1990), which are based on the impedance analysis of Kraft (1987), the same theory used for the VNA data. These internal calculations were used to determine ε' and ε'' at 50 MHz (without temperature correction) and σ_{dc}. In addition, σ' and σ'' at 50 MHz were back-calculated from ε' and ε'':

$$\sigma^* = \varepsilon^* \pi f \varepsilon_v \arctan\left(\frac{2\varepsilon''}{\varepsilon'}\right) \qquad [8]$$

where σ^* and ε^* are both for 50 MHz. Equation [8] is essentially the inverse of Eq. [3c]. This was done because the internal Hydra Probe calculations ignored ε_{rel}'' (Seyfried et al., 2005) (the ε'' portion of Eq. [1]). Kelleners et al. (2005) and Logsdon (2005) have shown that many soils have a bound-water ε_{rel}'' at 50 MHz, even though free-water relaxation is limited to much higher frequencies. The σ' (50 MHz) from Eq. [8] was assumed to be σ_{dc}; then ε_{rel}'' was determined from Eq. [1]. Because σ' would be slightly higher than σ_{dc}, the calculated ε_{rel}'' would be a little lower than that based on σ_{dc}.

The soil θ was linearly regressed against the ε' value determined by the Hydra Probe. The RMSE was determined as a measure of agreement between values of predicted (θ_p) and measured (θ_m) soil water contents:

$$\mathrm{RMSE} = \sqrt{\frac{\sum(\theta_m - \theta_p)^2}{n}} \qquad [9]$$

where n is the number of samples and Σ denotes summation from 1 to n.

Preliminary Study with Fluids

Preliminary studies examined the accuracies of the 12-wire–VNA system and the Hydra Probe based on measurements in fluids (Logsdon, 2005) of air, methanol (Fellner-Feldegg, 1969; Baker-Jarvis et al., 1998), isopropanol (Baker-Jarvis et al., 1998), and NaCl solutions from 0.005 to 0.020 mol L^{-1} (Stogryn, 1971). The reason for including measurement in fluids was because the fluid properties are well characterized in the literature, whereas soil water properties are not as definitively characterized. The ε' and ε'' of the Hydra Probe and 12-wire probe were compared with theoretical values for weak salt solutions and other fluids.

Procedure for Soil

For each location, soil, and vegetation group, soil cores were measured under refrigeration (4–7°C) and at room temperature (18–22°C). The soil temperatures were measured by the Hydra Probe and by a thermocouple (copper constantan) in a third soil core. The temperature range for the soils was broader than for the fluids because soil analyses were performed during 2 yr, but the fluid analyses were completed in 1 d. All measurements were determined across a range of θ, depending on the initial θ and density of each sample. The soil θ was changed by adding water to the sample and allowing equilibration for 1 h. Measurements were made at three to eight values of θ, depending on the initial θ. Some wetter samples were allowed to dry for 1 d at room temperature to slightly extend the θ range. Some of the samples in Idaho were marginally water repellent, which might have led to uneven wetting.

At each θ, the combined 12-wire probe and sample was weighed. The Hydra Probe samples were only weighed at the beginning and end to prevent disruption of the sample. The 12-wire sample masses were used to help estimate intermediate masses for the Hydra Probe samples. Subsamples of the cores before and after analysis were used to determine gravimetric water contents. The deficit (for samples not completely filled) or swelled core length was measured to compute the soil volume and the volumetric water contents.

Air-dry subsamples were used to determine the sorbed water content (Logsdon, 2005). First, the loose sample was placed into a vapor-tight container over distilled water (~99% relative humidity) for 2 to 3 wk, then over a saturated solution of $MgNO_3$ (~54% relative humidity) for 2 to 3 wk. Gravimetric water content was determined by weighing the soil sample, oven drying, and weighing again. The sorbed water content was determined for one or two subsamples from each core sample. The measured sorbed water content was multiplied by the bulk density or the original core sample to get the volumetric bound-water content (θ_b).

Occasionally data were missing due to errors such as incorrect VNA daily calibration (open + short + load), which invalidated the readings for the day, inadequate sample volume for analysis, or a missing data record for one θ in a sample. Because the samples were field moist, a wide range of θ values was not always possible. Most of the samples were undisturbed cores, so actual ranges of θ were not easily controlled. Therefore, for comparisons between samples (for the 12-wire probe with VNA and the Hydra Probe), values were interpolated at water content increments of 0.05 $m^3\ m^{-3}$. The cores were matched at these interpolated θ values by site, vegetation, and soil for comparison between methods. The RMSE was used to evaluate the comparisons between theory and measurement, and between different probes when theoretical values were not known.

To check for temperature effects, the interpolated data were paired by temperature within site, crop, and soil for each θ pair and each probe. The paired differences were pooled across the sites, and were considered significant if the 95% confidence interval did not include zero (Karlen and Colvin, 1992; Logsdon, 2008b).

By pooling data, θ(ε') was described as a third-order polynomial. At higher *f*, θ is often given as a linear relation with $\varepsilon'^{1/2}$; however, at lower *f*, θ may be linear with ε' instead (Schaap et al., 2003). Linear regression and correlation were determined for each sample that had more than three θ values, both for θ(ε') and for $\theta(\varepsilon'^{1/2})$. Then the slope of the θ(ε') was compared with the sorbed water values.

RESULTS AND DISCUSSION

Comparisons with Theory and between Probes

The ε' values reported by the Hydra Probe were biased high, compared with theoretical values for fluids, but correlated well (Fig. 3). The RMSE was 9.4, which was about a 9% error. The ε' values determined by the Hydra Probe were fairly close to the theoretical values for fluids (Fig. 4). The RMSE was 3.6, which was about a 4% error. The measured bias could be corrected by regression through the origin (not shown): $\varepsilon''_{theory} = 0.84\varepsilon''_{measured}$, and $\varepsilon'_{theory} = 0.96\varepsilon'_{measured}$. Blonquist et al. (2005) observed ε' values slightly lower than theoretical for fluids, especially at higher σ_{dc}, and Seyfried et al. (2005) observed ε' values close to theory.

The fluid σ_{dc} values were similar to theoretical values for both the 12-wire probe–VNA system and the Hydra Probe (Fig. 5), but

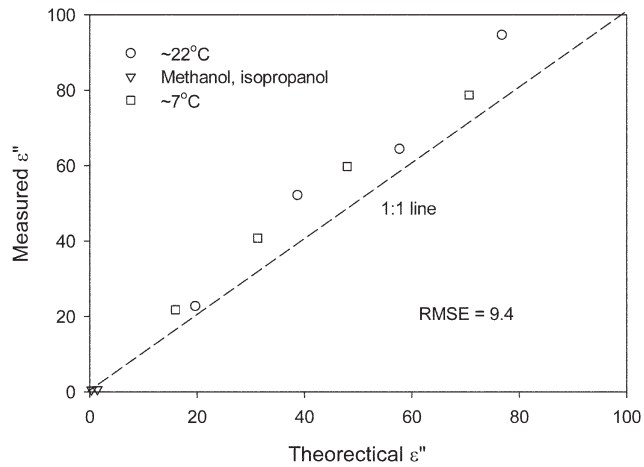

Fig. 3. Theoretical imaginary permittivity (ε") values compared with those determined using the Hydra Probe for different fluids, including salt solutions, at the given temperatures.

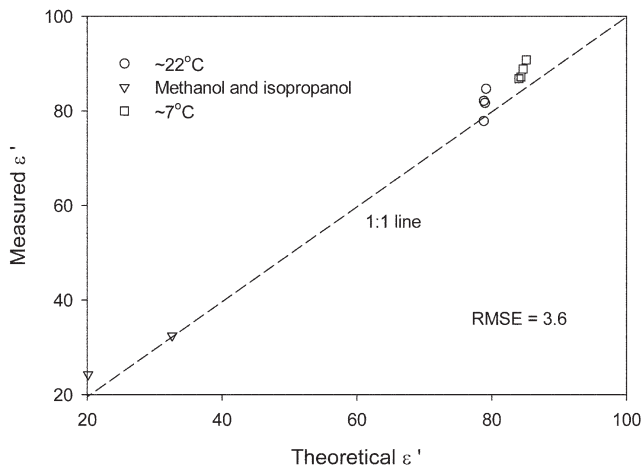

Fig. 4. Theoretical real permittivity (ε') values compared with those determined using the Hydra Probe for different fluids, including salt solutions, at the given temperatures.

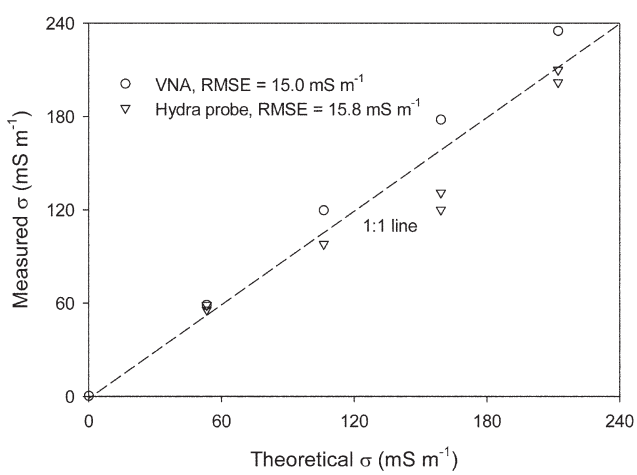

Fig. 5. Theoretical electrical conductivity (σ) values compared with those determined using the 12-wire probe connected to the vector network analyzer (VNA) or with the Hydra Probe.

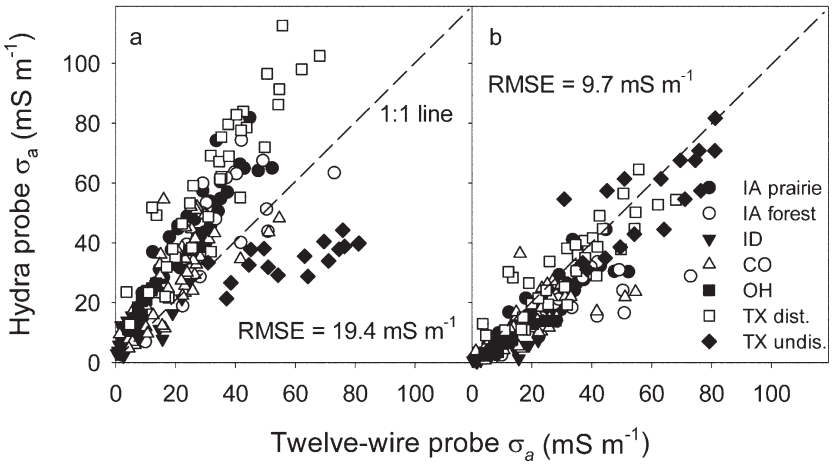

Fig. 6. Comparison of apparent soil electrical conductivity (σ_a) determined using the 12-wire probe connected to the vector network analyzer or using the Hydra Probe internal calculation (left) or the corrected Hydra Probe calculation (right). All cores for Iowa, Idaho, Colorado, and Ohio were undisturbed samples.

the VNA-derived values were biased high since they were at 300 kHz rather than direct current, and the Hydra Probe values were biased low. The bias could be corrected with regression through the origin (not shown): for the VNA, $\sigma_{theory} = 0.90\sigma_{measured}$; for the Hydra Probe, $\sigma_{theory} = 1.10\sigma_{measured}$. The RMSE for the 12-wire probe used with the VNA system was 15.0 mS m^{-1}, and the RMSE was 15.8 mS m^{-1}for the Hydra Probe, which is about a 6% error.

In contrast, the soil apparent σ_{dc} values were generally much higher when determined by the Hydra Probe than those from the 12-wire–VNA system, except for some Texas samples (Fig. 6a). The reason that some undisturbed Texas samples varied was vertically non-uniform soil θ because infiltration was hindered. The RMSE was 19.4 mS m^{-1}, or about a 16% error. The internal calculations for the Hydra Probe assume that ε" is only due to σ_{dc}, ignoring the ε_{rel}" contribution at 50 MHz. Ignoring ε_{rel}"would inflate the calculated σ_{dc} for these soils, but would not be obvious for salt solutions, which only have relaxation at higher *f*. Overall, the agreement between the Hydra Probe and the VNA was improved by using the back-calculation (Eq. [8], Fig. 6b). The RMSE was reduced to 9.7 mS m^{-1}, or about an 8% error. The back-calculated ε_{rel}" from Eq.[1] (total ε" minus the σ_{dc} component from Eq. [8]), was significantly ($P < 0.05$) related to θ_b ($r^2 = 0.27$) and the free-water component, θ_f ($r^2 = 0.53$), from stepwise regression analysis:

$$\varepsilon_{rel}'' = -6.55 + 22.3\theta_f + 161\theta_b \qquad [9]$$

Table 3. Correlation coefficients for the relation of free water or bound water with natural log of the characteristic frequency, f_c.

Group†	Free water	Bound water
Low f_c, cool	0.12	0.18
Low f_c, RT	0.21	0.06
High f_c, cool	0.34	0.06
High f_c, RT	0.27	0
Peak f_c, cool	0.50	0.09
Peak f_c, RT	0.50	0

† Low f_c is for exponent $n < 1$ and high f_c is for exponent $n = 1$; peak f_c is the shift from $n < 1$ to $n = 1$. RT is room temperature (18–22°C) and cool is refrigerated (4–7°C).

The θ_f was determined as total water minus θ_b. The sorbed water (used to calculated θ_b) would be related to surface area; a larger surface area indicates large colloid content, i.e., certain clays and organic matter. The Texas soils had the largest sorbed water value, and some of the Iowa soils had the next highest values (Table 1). The relation between the ε_{rel}" and θ_b (Eq. [9]) suggested that bound-water relaxation processes were important for many of these soils.

The bound-water relaxation processes (such as proton hopping) would be expected to vary as a function of *f*. In our study, the *f* range for ε* from the VNA was too narrow because the lowest possible *f* was 300 KHz and because the longer probe limited the usefulness of the data at high *f* (Logsdon, 2008a,b).

The surrogate f_c values fitted from Eq. [7] were interrelated with the fitted exponent, *n*. At higher θ and higher σ_{dc} values, the fitted *n* was at its maximum value of 1, which caused a decline in the fitted f_c at higher θ for that sample. On a per-sample basis, the peak fitted f_c as a function of θ occurred when the corresponding fitted *n* changed from <1 to 1. Both below and above the peak (largest) f_c values, the f_c values were only marginally, yet significantly ($P < 0.05$), related to both free and bound water (Table 3). The peak f_c values were more strongly related to θ_b than were the values lower or higher than the peak. The f_c values were lower than the resonance f_R from which ε_a had been calculated, so temperature could have an influence (de Loor, 1968).

The apparent σ' at 300 kHz for the 12-wire–VNA system agreed well with the values fitted using Eq. [7] (Fig. 7). The RMSE was 3.0 mS m^{-1}, which was about a 4% error. Overall, the two σ' values were comparable, but σ' determined at 300 kHz was biased high for σ' values >25 mS m^{-1}. The fitted *n* has a maximum of 1, as stated above, which resulted in the fitted σ values being high at large θ. Except for this bias, the trend was expected because σ' increases as *f* increases. Comparing $\varepsilon_a^{1/2}$ at the f_R with

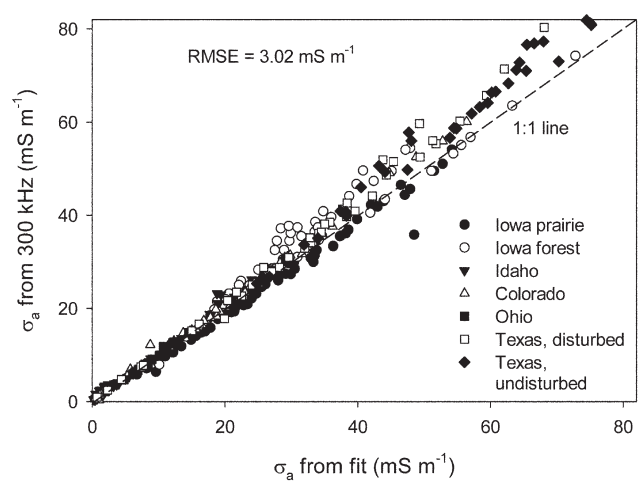

Fig. 7. The apparent electrical conductivity (σ_a) at 300 kHz for the 12-wire probe connected to the vector network analyzer system vs. the values fitted using Eq. [8].

that from the Hydra Probe at 50 MHz showed that $\varepsilon_a^{1/2}$ was often higher for the Hydra Probe than for the 12-wire–VNA system (Fig. 8). The RMSE was 0.59, or about an 8% error.

Pooling all the Hydra Probe data together produced a fitted curve for θ as a function of ε' with an RMSE of 0.046 $m^3\ m^{-3}$ (Fig. 9). This rather large uncertainty might be reduced by site-specific calibration. The regression equation through the origin was

$$\theta = 0.0224\varepsilon' - 0.00047\varepsilon'^2 + 0.00000514\varepsilon'^3 \quad [10]$$

Considering each sample separately, the regression of θ(ε') was significantly correlated ($P < 0.05$) for all but three samples. The three samples that were not significant at the 0.05 level were significant at $P < 0.10$. For all but two of these samples, the correlation was stronger with ε' than with $\varepsilon'^{1/2}$. The slope, Δθ/Δε', as a function of sorbed water (kg kg^{-1}) showed that above 0.04 kg kg^{-1} sorbed water, the slope was lower with little variability (Fig. 10). High sorbed water indicated high surface area and was associated with higher ε', so the corresponding slope, Δθ/Δε', was lower. For sorbed water <0.04 kg kg^{-1}, the slope was larger and varied considerably. The variation in slope for low sorbed water was not encouraging for finding a unified calibration equation for the Hydra Probe.

Temperature Effects

As expected, σ' was significantly higher at room temperature than with refrigerated samples, both for the Hydra Probe corrected values and for those determined from the 12-wire–VNA system (not shown). The $\varepsilon_a^{1/2}$ determined from the 12-wire probe was also significantly larger at room temperature than at the refrigerated temperature. The ε' determined from the Hydra Probe was not significantly affected by temperature, but ε_{rel}'' was significantly higher at room temperature than at the refrigerated temperature.

CONCLUSIONS

Both the Hydra Probe and the 12-wire probe provided fairly accurate ε* and σ* values of fluids. The soil σ' from the Hydra Probe was improved when back-calculated from ε' and ε'' (Eq. [8]). This back-calculated σ' (50 MHz) was lower in value than the σ_{dc} calculated with the Hydra Probe software; however, theory requires the σ_{dc} to be smaller than that determined at any alternating current *f*. Inherent in the Hydra Probe software is the assumption that all ε'' was due to σ_{dc}, ignoring ε_{rel}'', and this incorrect assumption was the main source of error. This would not be a problem for fluids nor for soils with minimal bound water (i.e., sand). Thus bound-water relaxation could not be neglected for the soils tested here.

Overall, electrical properties did not show promise for distinguishing soil and management features. Soils with larger amounts of sorbed water had a small slope for the θ(ε') relation because ε' was increased for these soils; soils with less sorbed water had larger variability in the slope of θ(ε').

Measurements on undisturbed samples were not always possible for dense samples or for samples with layers that restricted water movement. Uneven wetting might have been indicated for samples that had water-repellent surface layers; however, water repellency was only tested on sieved soil after determining the

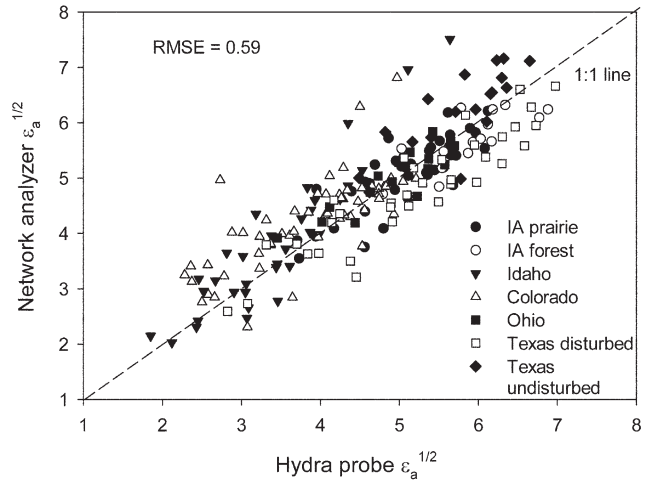

Fig. 8. Comparison of the $\varepsilon_a^{1/2}$ (square root of apparent permittivity) of the 12-wire probe connected to the vector network analyzer at the resonance frequency with that of the Hydra Probe at 50 MHz.

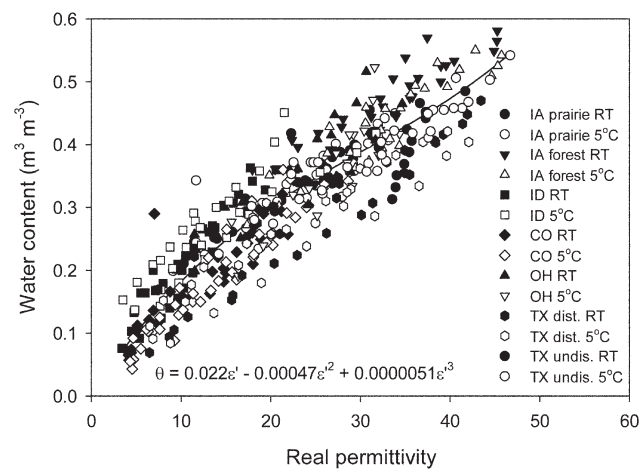

Fig. 9. Water content (θ) as a function of the real permittivity (ε') determined by the Hydra Probe for soils from six locations (RT is room temperature). All cores for Iowa, Idaho, Colorado, and Ohio were undisturbed samples.

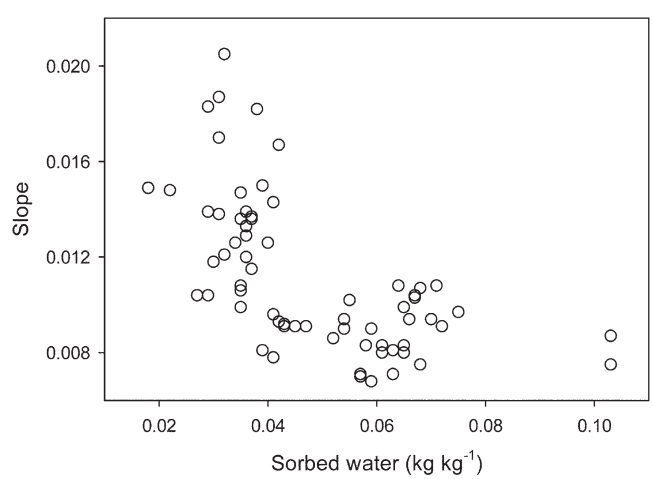

Fig. 10. The slope of the water content as a function of the real permittivity [θ(ε')] is determined first, shown here as a function of the sorbed water content.

electrical properties. Possible uneven wetting might have contributed to low values of electrical properties for some Idaho samples compared with other samples from the same location. For many samples, the θ range was inadequate for detecting trends with θ. Sieved and repacked samples might be more appropriate for testing electrical properties across a range of θ values, temperatures, densities, soils, and management practices.

ACKNOWLEDGMENTS

We acknowledge Gavin Simmons for sample collection in Iowa and processing samples, Robert Erskine for assistance with the Colorado sample site selection and soil sampling, and Brice Ruthardt for assistance with the Texas sampling. We thank Scott Jones and Thijs Kelleners for helpful comments on an early version of this manuscript.

REFERENCES

Baker-Jarvis, J., M.D. Janezic, and C.A. Jones. 1998. Shielded open-circuited sample holder for dielectric measurement of solids and liquids. IEEE Trans. Instrum. Meas. 47:338–344.

Berberian, J.G., and E. King. 2002. An overview of time domain spectroscopy. J. Non-Cryst. Solids 305:10–18.

Bialkowski, S.E., L. Dudley, and D. Or. 2002. Using an expectation-maximization algorithm to obtain dielectric relaxation-time spectra of aqueous montmorillonite clay suspensions. Appl. Spectrosc. 56:1470–1474.

Blonquist, J.M., Jr., S.B. Jones, and D.A. Robinson. 2005. Standardizing characterization of electromagnetic water content sensors: 2. Evaluation of seven sensing systems. Vadose Zone J. 4:1059–1069.

Campbell, J.E. 1990. Dielectric properties and influence of conductance in soils at one to fifty megahertz. Soil Sci. Soc. Am. J. 54:332–341.

de Loor, G.P. 1968. Dielectric properties of heterogeneous mixtures containing water. J. Microw. Power 3–2:67–73.

Evett, S.R., R.C. Schwartz, J.A. Tolk, and T.A. Howell. 2009. Soil profile water content determination: Spatiotemporal variability of electromagnetic and neutron probe sensors in access tubes. Vadose Zone J. (in press).

Evett, S.R., J.A. Tolk, and T.A. Howell. 2005. Time domain reflectometry laboratory calibration in travel time, bulk electrical conductivity, and effective frequency. Vadose Zone J. 4:1020–1029.

Evett, S.R., J.A. Tolk, and T.A. Howell. 2006. Soil profile water content determination: Sensor accuracy, axial response, calibration, temperature dependence, and precision. Vadose Zone J. 5:894–907.

Fellner-Feldegg, H. 1969. The measurement of dielectrics in the time domain. J. Phys. Chem. 73:616–623.

Green, T.R., G.H. Dunn, R.H. Erskine, J.D. Salas, and L.R. Ahuja. 2009. Fractal analyses of steady infiltration and terrain on an undulating agricultural field. Vadose Zone J. 8:310–320.

Heimovaara, T.J., E.J.G. de Winter, W.K.P. van Loon, and D.C. Esveld. 1996. Frequency-dependent dielectric permittivity from 0 to 1 GHz: Time domain reflectometry measurements compared with frequency domain network analyzer measurements. Water Resour. Res. 32:3603–3610.

Hunt, A.G., S.D. Logsdon, and D.A. Laird. 2006. Charge transfer in humidified smectite clays. Soil Sci. Soc. Am. J. 70:14–23.

Ishida, T., M. Kawase, K. Yagi, J. Yamakawa, and K. Fukada. 2003. Effects of the counterion on dielectric spectroscopy of a montmorillonite suspension over the frequency range 105–1010 Hz. J. Colloid Interface Sci. 268:121–126.

Ishida, T., and T. Makino. 1999. Effects of pH on dielectric relaxation of montmorillonite, allophane, and imogolite suspensions. J. Colloid Interface Sci. 212:152–161.

Karlen, D.L., and T.S. Colvin. 1992. Alternative farming system effects on profile nitrogen concentrations on two Iowa farms. Soil Sci. Soc. Am. J. 56:1249–1256.

Kelleners, T.J., D.A. Robinson, P.J. Shouse, J.E. Ayars, and T.H. Skaggs. 2005. Frequency dependence of the complex permittivity and its impact on dielectric sensor calibration in soils. Soil Sci. Soc. Am. J. 69:67–76.

Kraft, C. 1987. Constitutive parameter measurements of fluids and soil between 500 kHz and 5 MHz using a transmission line technique. J. Geophys. Res. 92:10650–10656.

Logsdon, S.D. 2005. Soil dielectric spectra from vector network analyzer data. Soil Sci. Soc. Am. J. 69:983–989.

Logsdon, S.D. 2008a. Activation energies and temperature effects from electrical spectra of soil. Soil Sci. 173:359–367.

Logsdon, S.D. 2008b. Electrical spectra of undisturbed soil from crop rotation study. Soil Sci. Soc. Am. J. 72:11–15.

Logsdon, S.D. 2009. CS616 calibration: Field versus laboratory. Soil Sci. Soc. Am. J. 73:1–6.

Logsdon, S.D., and B. Hornbuckle. 2006. Soil moisture probes for dispersive soils. Pap. 13. *In* TDR 2006: Int. Symp. and Worksh. on Time Domain Reflectometry for Innovative Soils Applications, 3rd, West Lafayette, IN. Sept. 2006. Available at engineering.purdue.edu/TDR/Papers/13_Paper.pdf (verified 16 Oct. 2009). Purdue Univ., W. Lafayette, IN.

McCoy, A.J., G. Parkin, C. Wagner-Riddle, J. Warland, J. Lauzon, P. van Bertoldi, D. Fallow, and S. Jayasundara. 2006. Using automated soil water content measurements to estimate soil water budgets. Can. J. Soil Sci. 86:47–56.

McCutcheon, M.C., H.J. Farahani, J.D. Stednick, G.W. Buchleiter, and T.R. Green. 2006. Effect of soil water on the apparent soil electrical conductivity and texture relation in a dryland field. Biosyst. Eng. 94:19–32.

Poinsignon, C. 1997. Protonic conductivity and water dynamics in swelling clays. Solid State Ionics 97:399–407.

Raythatha, R., and P.N. Sen. 1986. Dielectric properties of clay suspensions in MHz to GHz range. J. Colloid Interface Sci. 109:301–309.

Robinson, D.A., S.B. Jones, J.M. Blonquist, Jr., and S.P. Friedman. 2005. A physically derived water content/permittivity calibration model for coarse-textured, layered soils. Soil Sci. Soc. Am. J. 69:1372–1378.

Schaap, M.G., D.A. Robinson, S.P. Friedman, and A. Lazar. 2003. Measurement and modeling of the TDR signal propagation through layered dielectric media. Soil Sci. Soc. Am. J. 67:1113–1121.

Schwan, H.P. 1966. Alternating current electrode polarization. Biophysik 3:181–201.

Schwartz, R.C., S.R. Evett, M.G. Pelletier, and J.M. Bell. 2009a. Complex permittivity model for time domain reflectometry soil water content sensing: I. Theory. Soil Sci. Soc. Am. J. 73:886–897.

Schwartz, R.C., S.R. Evett, M.G. Pelletier, and J.M. Bell. 2009b. Complex permittivity model for time domain reflectometry soil water content sensing: II. Calibration. Soil Sci. Soc. Am. J. 73:898–909.

Seyfried, M.S., and L.E. Grant. 2007. Temperature effects on soil dielectric properties measured at 50 MHz. Vadose Zone J. 6:759–765.

Seyfried, M.S., L.E. Grant, E. Du, and K. Humes. 2005. Dielectric loss and calibration of the Hydra Probe soil water sensor. Vadose Zone J. 4:1070–1079.

Seyfried, M.S., and M.D. Murdock. 2004. Measurement of soil water content with a 50-MHz soil dielectric sensor. Soil Sci. Soc. Am. J. 68:394–403.

Shang, J.Q., R.K. Rowe, J.A. Umana, and J.W. Scholte. 1999. A complex permittivity measurement system for undisturbed/compacted soils. Geotech. Test. J. 22:159–168.

Soil Survey Staff. 2008. Official soil series descriptions. Available at soils.usda.gov/technical/classification/osd/index.html (accessed 10 July 2008; verified 16 Oct. 2009). NRCS, Lincoln, NE.

Stogryn, A. 1971. Equations for calculating the dielectric constant of saline water. IEEE Trans. Microw. Theory Tech. 19:733–736.